Preprints of the 19th World Congress
The International Federation of Automatic Control
Cape Town, South Africa. August 24-29, 2014

State bounds estimation for nonlinear systems using μ-analysis ⋆

Jongrae Kim * **Masako Kishida** ** **Declan G. Bates** ***

* *Biomedical Engineering/Aerospace Sciences, University Avenue, University of Glasgow, Glasgow G12 8QQ, UK (e-mail: Jongrae.Kim@glasgow.ac.uk).*
** *Electrical & Computer Engineering, University of Canterbury, Christchurch, New Zealand (e-mail: masako.kishida@canterbury.ac.nz)*
*** *School of Engineering, University of Warwick, Coventry CV4 7AL, UK (e-mail: D.Bates@warwick.ac.uk)*

Abstract: Developing state bound estimation algorithms for nonlinear systems has been of high importance in robustness analysis of dynamic systems. For many cases, Monte-Carlo simulation might be the only tool to estimate these bounds for a general type of nonlinear systems. The required number of simulations for a tight bound, however, would be very large and it might be impossible to complete within a given computation time. μ-formulation for state bounds transforms the bound estimation problem to a singularity problem and the singular problem is solved using a randomised optimisation approach. The performance of the algorithms are demonstrated by a simple discrete system; large-scale biological systems; and a hybrid system.

Keywords: State bound estimation, Nonlinear discontinuous system

1. INTRODUCTION

Robustness analysis is an indispensable step in designing engineering systems (Balas et al., 2001; Ferreres and Biannic, 2001; Menon et al., 2006). It is also accepted now one of the most important aspects in analysing biological systems (Kitano, 2004; Wagner, 2005; Gilchrist et al., 2006; Kim et al., 2006; Shinar et al., 2007; Clodong et al., 2007; Acar et al., 2008). Systematic approach to model biological interactions and analyse measurement data is one of the highly preferable ways in improving our understanding of complex systems (Kholodenko et al., 2002; Hoehndorf et al., 2011). Recently, some of the models are described with many states and parameters of several hundreds (Kuhn et al., 2009; Chen et al., 2009) and these provide information that was not available with small scale models. Similarly, current engineering systems become more and more complex and this tendency will continue in future. Hence, it is important to have an efficient numerical methods to analyse these large-scale systems.

Structured singular value or μ-analysis has been one of the most successful tools for robustness evaluation (Doyle, 1982; Skogestad and Postlethwaite, 1996; Kao et al., 2001; Cantoni and Glover, 2000). Even though the computational complexity of μ-analysis was acknowledged, it has been successfully used for many practical systems design and analyses.

The computational complexity proof in Braatz et al. (1994) is performed by transforming μ problem to a corresponding optimisation problem that is known to be NP-hard. As far as NP≠P, the computational complexity is a fundamental obstacle that cannot be overcome by any traditional algorithms. However, practically μ-analysis algorithm produced many useful results and recently, it is further extended to solve some class of optimisation problems efficiently (Kishida et al., 2011). This is an inverse interpretation of the formulation in Braatz et al. (1994). The application in Kishida et al. (2011) is calculating state bounds for polynomial nonlinear discrete systems, where initial states and parameters in the systems are given with known uncertain bounds. Then, the state maximum and minimum bounds are calculated using μ upper and lower bounds algorithms. As long as the nonlinearity appears in polynomial formats, the uncertainties can be decoupled from the known parts and the system can be described in Linear Fractional Transformation (LFT) (Braatz et al., 1994; Doyle et al., 1989). Once it is in LFT form, then there are some powerful numerical tools that provide the upper and the lower bounds of μ (Balas et al., 2001).

Conservatism of the calculated bounds and the requirement for the uncertainty structures for enabling LFT format are two main obstacles for the state bounds algorithm to be further extending its applications. μ-analysis problem is interpreted in geometrical point of view in Kim et al. (2009) and it enables one to use random sampling approach to obtain the bounds. Later, it is further lifted the requirement of LFT-transformation, i.e. LFT-free μ-analysis (Zhao et al., 2011). It is, hence, a natural fusion that combining the state bounds estimation and the LFT-free μ-analysis. Calculating the bounds of a polynomial function using the skewed μ-analysis framework presented in Kishida et al. (2011) is extended to a general type of nonlinear systems, including dis-continuous and

⋆ This research was supported by EOARD (European Office of Aerospace Research & Development), the grant number US-EURO-LO (FA8655-13-1-3029).

non-smooth nonlinear functions using a random sampling method (Zhao et al., 2011).

This paper is organised as follows: Firstly, state bounds estimation problem is formulated as LFT-free μ-analysis. Secondly, state worst-bounds algorithms are presented. Thirdly, the algorithm is parallelised to run on GPU (Graphical Processing Unit) and its performance is demonstrated using three examples: an oscillatory discrete system; a large-scale biological system and a hybrid system. Finally, the conclusions are presented.

2. STATE BOUNDS IN LFT-FREE μ-FORMULATION

A nonlinear dynamical system is given by

$$\dot{x} = f(x, p), \tag{1}$$

where the initial conditions are $x_0 = x(0)$, $\dot{x}$ is the time-derivative of x, x is the state vector, an element of the set, $\mathbb{R}^{n_x}$, $\mathbb{R}^{n_x}$ is the n_x-dimensional real space, n_x is a positive integer, p is the uncertain parameters, an element of $\mathbb{R}^{n_p}$, n_p is a positive integer, and $f(x, p)$ is a nonlinear function in x and p including dis-continuous functions and non-smooth functions. For the well-posedness of the problem, $f(x, p)$ is assumed to give a unique solution for the nonlinear differential equation. For a chosen positive real number, Δt, a transition function $\phi(,)$ is defined to satisfy the following:

$$x_{k+1} = \phi(x_k, p) \tag{2}$$

where $x_k = x(k\Delta t)$ for $k = 0, 1, 2, \ldots$. The problem is finding the worst-bounds for the maximum and the minimum of the state, x_{k+1}, for the given bounds for x_0 and p. For brevity, we consider a scalar case for x and p only but the general formulation for the multi-dimensional x and p is exactly the same as shown in below.

Problem 1. (state bounds estimation) Calculate $\underline{\phi}_{\min}$, $\bar{\phi}_{\min}$, $\underline{\phi}_{\max}$ and $\bar{\phi}_{\max}$ in the following inequalities:

$$\underline{\phi}_{\min} \le \underline{\phi} \le \bar{\phi}_{\min}, \tag{3a}$$

$$\underline{\phi}_{\max} \le \bar{\phi} \le \bar{\phi}_{\max}, \tag{3b}$$

where $\underline{\phi} \le \phi(x_k, p) \le \bar{\phi}$, $\underline{x}_0 \le x_0 \le \bar{x}_0$, $\underline{p} \le p \le \bar{p}$, and all the upper and the lower bounds for $\phi(x_k, p)$, x_0 and p are finite.

By solving problem 1 we are to find state boundaries for x_{k+1} for the give uncertain values for the initial condition and the parameters in the dynamical system. A special case of the problem, where ϕ is a polynomial function in x_k and p, can be transformed into LFT form and existing μ bounds algorithms can be directly used to obtain the bounds. Details about the special case can be found in Kishida et al. (2011). Although Problem 1 is more general than the one in Kishida et al. (2011), the main idea obtaining the state bounds using μ-formulation is the same but exploiting the LFT-free formulation in Zhao et al. (2011), which will be presented in the following.

Consider the case that each x_0 and p can be written as

$$x_0 = x_c + w_x \delta_x \tag{4a}$$

$$p = p_c + w_p \delta_p \tag{4b}$$

where $x_c = (\underline{x}_0 + \bar{x}_0)/2$, $p_c = (\underline{p} + \bar{p})/2$, and w_x or w_p is a weight to define the boundary of x_0 or p such that δ_x or δ_p is given by

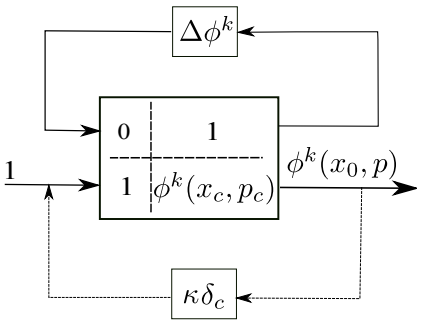

Fig. 1. Pseudo-LFT form

$$-1 \le \delta_x \le 1 \tag{5a}$$

$$-1 \le \delta_p \le 1 \tag{5b}$$

In order to lift the polynomial function requirement on $\phi(x_k, p)$, define

$$\Delta\phi^k(\delta_x, \delta_p) := \phi^k(x_0, p) - \phi^k(x_c, p_c) \tag{6}$$

where

$$\phi^k(\cdot, p) := \underbrace{\phi \circ \phi \circ \phi \circ \ldots \circ \phi}_{k\text{-times}}(\cdot, p) \tag{7}$$

and

$$\phi^2(\cdot, p) = \phi \circ \phi(\cdot, p) = \phi[\phi(\cdot, p), p] \tag{8}$$

Now, a pseudo-LFT form as shown in Figure 1 is to be constructed. It is called a pseudo-LFT as it is in the LFT format but it can be only evaluated for a fixed δ_x and δ_p. In the standard LFT-formulation, $\Delta\phi^k$ is a constant matrix with a structure. On the other hand, in the pseudo-LFT formulation, it is a varying vector depending on the values of δ_x and δ_p.

From the pseudo-LFT shown in Figure 1 and the equivalency between μ-bounds and the optimisation problem shown in Braatz et al. (1994), the maximum of $|\phi^k(x_0, p)|$ is bounded above as

$$\max |\phi^k(x_0, p)| \le \frac{1}{\kappa^*} \tag{9}$$

where κ^* is the minimum κ among the ones satisfy the singular condition:

$$|I_2 - N\Delta| = 0, \tag{10}$$

$|\cdot|$ is the determinant of matrix, I_2 is the 2×2 identify matrix,

$$N = \begin{bmatrix} 0 & 1 \\ 1 & \phi^k(x_c, p_c) \end{bmatrix}, \tag{11a}$$

$$\Delta = \begin{bmatrix} \Delta\phi^k & 0 \\ 0 & \kappa\delta_c \end{bmatrix}, \tag{11b}$$

$|\delta_c| = |\delta_R + \delta_I j| \le 1$, δ_R and δ_I are the real numbers whose magnitude is less than or equal to 1, and $j = \sqrt{-1}$.

The singularity condition is expanded

$$\begin{aligned} |I_2 - N\Delta| &= \begin{vmatrix} 1 & -\kappa\delta_c \\ -\Delta\phi^k & 1 - \kappa\phi^k(x_c, p_c)\delta_c \end{vmatrix} \\ &= 1 - \kappa\phi^k(x_c, p_c)\delta_c - \kappa\Delta\phi^k\delta_c \\ &= \left\{1 - \kappa\left[\phi^k(x_c, p_c) + \Delta\phi^k\right]\delta_R\right\} \\ &\quad - \kappa\left[\phi^k(x_c, p_c) + \Delta\phi^k\right]\delta_I j = 0 \end{aligned} \tag{12}$$

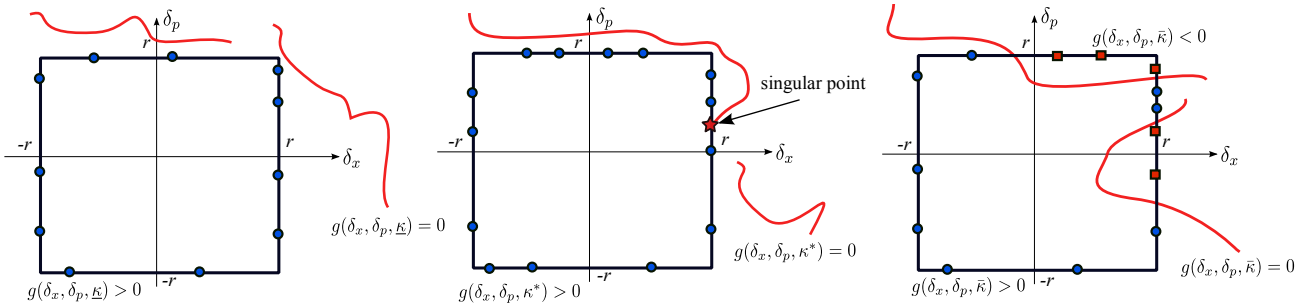

Fig. 2. Sign changes along the uncertain box boundary: as $\underline{\kappa}$ is smaller than κ^*, all signs of $g(\delta_x, \delta_p, \underline{\kappa})$ for the samples at the boundary are positive; on the other hand, when $\bar{\kappa}$ is greater than κ^*, there are red box samples and blue circle samples whose sign of $g(\delta_x, \delta_p, \bar{\kappa})$ is positive and negative, respectively.

The following is the only singular condition:

$$1 - \kappa \left[\phi^k(x_c, p_c) + \Delta\phi^k\right] \delta_R = 0, \text{ and } \delta_I = 0 \qquad (13)$$

i.e., the imaginary value of δ_c is always equal to zero. Notice also that $\phi^k(x_c, p_c) + \Delta\phi^k$ is equal to $\phi^k(x_0, p)$ by the definition. Therefore, the minimum κ, i.e. κ^*, occurs at the following condition:

$$\kappa^* = \frac{1}{\max[\phi^k(x_0, p)\delta_R]} = \frac{1}{\max|\phi^k(x_0, p)|} \qquad (14)$$

where $\delta_R = \pm 1$. This looks trivial and it does not seem to help to find the bounds for $\phi^k(x_0, p)$. In the next section, a random sampling approach to solve the above problem, which could be interpreted as a multi-dimensional bi-section method.

3. WORST BOUNDS ESTIMATION

Define

$$g(\delta_x, \delta_p, \kappa) := 1 - \kappa|\phi^k(x_c + W_x\delta_x, p_c + W_p\delta_p)| \qquad (15)$$

where $-r \le \delta_x \le r$, $-r \le \delta_p \le r$, $\kappa > 0$, and $r \in (0, 1]$. Note that $g(\cdot, \cdot, \cdot)$ could be dis-continuous as $\phi^k(\cdot, \cdot)$ could be dis-continuous. As shown in Figure 2, if $\bar{\kappa}$ is larger than κ^*, then there are two cases, i.e. either having two types of samples, whose signs are positive or negative, or having one type of sample, whose signs are all negative. Similarly, if only positive signs are found, then the corresponding κ is smaller than κ^*, which is the case that $\kappa = \underline{\kappa}$. Hence, the bound for κ^* is given by

$$\underline{\kappa} \le \kappa^* \le \bar{\kappa} \qquad (16)$$

where $\bar{\kappa}$ is a deterministic bound as we found the negative sign but $\underline{\kappa}$ is probabilistic as it has always some danger to be failed depending on the number of samples checked on the boundary.

Algorithm 1. Pre-$\underline{\kappa}$ estimation

(1) Set N, the number of samples along the face of the uncertain box shown in Figure 2
(2) Set the initial boundary for κ such that $\epsilon \le \kappa^* \le E$, where ϵ is equal to zero and E could be the largest number that can be expressed in computer.
(3) Set the tolerance, ε, for the magnitude of the interval, $[\epsilon, E]$, i.e. $E - \epsilon$
(4) Set $\kappa = (\epsilon + E)/2$, which is the initial guess of $\bar{\kappa}$.
(5) for $i = 1$ to N
- Evaluate $g(\delta_x, \delta_p, \kappa)$ for the given i-th sample of δ_k and δ_p
- if $g(\delta_x, \delta_p, \kappa) < 0$, then replace E by κ and break the for-loop, else continue the for-loop

(6) If $i = N$ and $g(\delta_k, \delta_p, \kappa)$ for all samples are positive, then replace ϵ by κ.
(7) If $E - \epsilon$ is smaller than ε, then declare $\underline{\kappa}_p = E$ and stop. Otherwise, go to step 4)

Note that $\underline{\kappa}_p$ from the pre-$\underline{\kappa}$ estimation algorithm does not need to be tight as long as it is smaller than κ^*. The reason to calculate $\underline{\kappa}_p$ using the above algorithm before actually obtaining any tight bounds for $\phi^k(x_0, p)$ is that the value of $\phi^k(x_0, p)$ can be positive and negative and the definition of κ^* in (14) is given in terms of the absolute value of $\phi^k(x_0, p)$.

In order to estimate the bounds for the maximum $\phi^k(x_0, p)$, the following is defined:

$$\bar{g}(\delta_x, \delta_p, \kappa) := 1 - \kappa|\phi^k(x_0, p) + s/\underline{\kappa}_p| \qquad (17)$$

where s is a safety factor, greater than 1. As $1/\underline{\kappa}_p > |\phi^k(x_0, p)|$ can be guaranteed only in a probabilistic sense, the safety factor will make sure the terms inside the absolute sign be positive. Then, the maximum of $|\phi^k(x_0, p) + s/\underline{\kappa}_p|$ occurs at $\bar{\phi}^k(x_0, p) + s/\underline{\kappa}$.

Algorithm 2. $\bar{\phi}$-bounds estimation Algorithm

(1) Run the pre-$\underline{\kappa}$ estimation algorithm after replacing $g(\delta_x, \delta_p, \kappa)$ by $\bar{g}(\delta_x, \delta_p, \kappa)$
(2) Set $\underline{\kappa} = \epsilon$ and $\bar{\kappa} = E$
(3) Declare $\underline{\phi}_{\max} = 1/\bar{\kappa} - s/\underline{\kappa}_p$ and $\bar{\phi}_{\max} = 1/\underline{\kappa} - s/\underline{\kappa}_p$

Similarly, to obtain the bounds for the minimum, define

$$\underline{g}(\delta_x, \delta_p, \kappa) := 1 - \kappa|\phi^k(x_0, p) - s/\underline{\kappa}_p| \qquad (18)$$

and run the following algorithm:

Algorithm 3. $\underline{\phi}$-bounds estimation Algorithm

(1) Run the pre-$\underline{\kappa}$ estimation algorithm after replacing $g(\delta_x, \delta_p, \kappa)$ by $\underline{g}(\delta_x, \delta_p, \kappa)$
(2) Set $\underline{\kappa} = \epsilon$ and $\bar{\kappa} = E$
(3) Declare $\underline{\phi}_{\min} = 1/\bar{\kappa} + s/\underline{\kappa}_p$ and $\bar{\phi}_{\min} = 1/\underline{\kappa} + s/\underline{\kappa}_p$

Finally, the above will be repeated for a different r in $(0, 1]$. It is worth to note that the suggested algorithm is different from the blind Monte-Carlo random searches. The search performs through random samples but each iteration it converges towards a solution with the speed of bisection method.

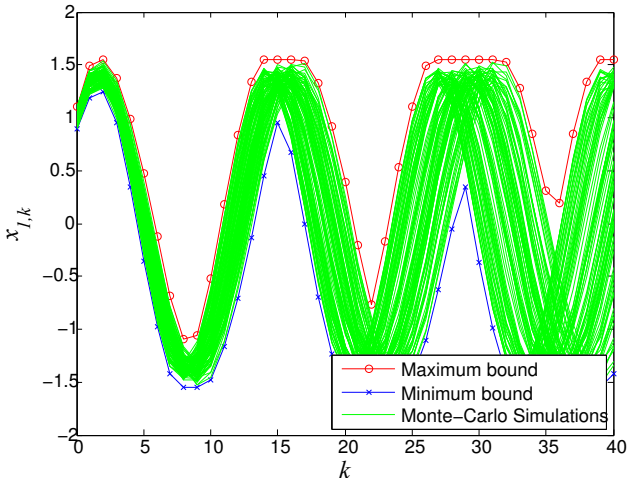

Fig. 3. Bounds for $x_{1,k}$

Remark 2. The total computational cost depends on how many times the algorithms are executed for different r in $(0, 1]$. If the upper bounds could be provided with less computation, the proposed algorithm could be used only for finding lower bounds.

The proposed three algorithms are *embarrassingly parallel*, i.e. all sampling evaluations are independent each other and no effort is required to parallelise the algorithms. Therefore, it is a perfect problem to be solved on GPU (Graphical Processing Unit). The algorithms are implemented using CUDA-GPU (NVIDIA Developer zone: NVIDIA, CUDA 5.0, 2013). In the following examples, the sampling evaluation part of the algorithms is running on NVIDIA Tesla C2050, which has 449 Cores and the maximum number of threads per block is 1024.

4. EXAMPLES

4.1 Oscillatory state

The following example is from Kishida et al. (2011):

$$\begin{bmatrix} x_{1,k+1} \\ x_{2,k+1} \end{bmatrix} = \phi(x_k, p) = \frac{1}{\sqrt{1+p^2}} \begin{bmatrix} 1 & p \\ -p & 1 \end{bmatrix} \begin{bmatrix} x_{1,k} \\ x_{2,k} \end{bmatrix} \quad (19)$$

Because of the polynomial format requirement of the algorithm in Kishida et al. (2011), $\sqrt{1+p_c^2}$ was used instead of $\sqrt{1+p^2}$. Here, it does not need to be polynomial and the original form, $\sqrt{1+p^2}$, is used. The intervals for the initial state and the uncertain parameters, p, are given as follows: $0.9 \leq x_{0,1} \leq 1.1$, $0.9 \leq x_{0,2} \leq 1.1$, and $0.45 \leq p \leq 0.55$.

The algorithm firstly calculates the pre upper bound for $|\phi|$, $1/\underline{\kappa}$, and set $s = 2$. Secondly, the bounds for $\max(\phi)$ and $\min(\phi)$ are obtained by the algorithm 2 and 3. Figure 3 shows the bounds for $x_{1,k}$, where $k = 1, 2, \ldots, 39, 40$. The upper and lower bounds of the maximum and the minimum for $r = 1$ shown in Figure 3 are very close to each other. All trajectories from random simulations are well bounded by the estimated bounds.

4.2 ErbB Signalling Pathways

ErbB or epidermal growth factor receptor related pathways are among the most extensively studied biological signalling networks (Chen et al., 2009). Abnormality of ErbB signalling pathways cause various human cancers (Engelman et al., 2007; Zhou et al., 2009; Yonesaka et al., 2011). In Chen et al. (2009), an ErbB mathematical model including 13 known ErbB ligands, EGF (Epidermal Growth Factor) and heregulin (HGF) and Erk and Akt pathways are presented. It has 504 states, 828 reactions and 226 kinetic parameters. The set of 504 differential equations is extracted from the simbiology model (Chen et al., 2009). It is known that this model is only valid up to a few hours and it is not necessary for this system to be stable for infinite time period. As long as the states remain in a certain bound, the network works perfectly as it should be. Hence, the required robustness analysis is obtaining the future state bounds with respect to the uncertain parameters.

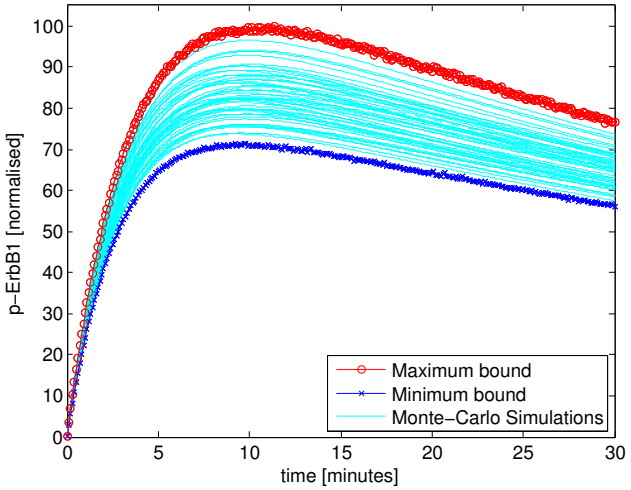

Fig. 4. Bounds for p-ErbB1 with respect to uncertainties in 226 kinetic parameters

One of the interesting biological features found in Chen et al. (2009) using the model is that parametric sensitivities of the dynamical system strongly depend on input condition. This could be the reason that it provides so diverse responses. Parametric uncertainties are introduced for those 226 kinetic parameters. The uncertainty ranges are set to $\pm 10\%$ from the nominal values. Among the several input conditions, the robustness is tested for the case of EGF equal to 5nM. The bounds for phospholilated ErbB1, i.e. p-ErbB1, is shown in Figure 4. Again, the upper and lower bounds for the maximum and the minimum are very close to each other and only the upper bounds for both are indicated. All trajectories from random simulations are well bounded by the estimated bounds.

4.3 Inverted Pendulum: Hybrid System

A switching controller for inverted pendulum stabilisation is shown in Åström and Furuta (2000). A simplified version of the system is given by

$$\ddot{\theta} = p \sin\theta - u \cos\theta \quad (20)$$

where θ is the angle of pendulum measured from the upright position, p is the uncertainty caused by some physical parameters and u is the control input. The total energy, E, including kinetic and potential energy is given by

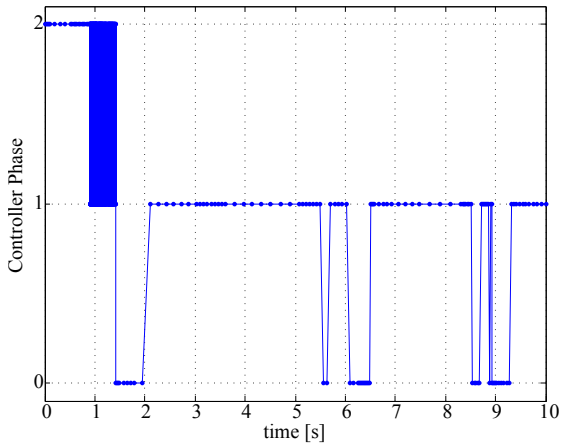

Fig. 5. Controller switching phase examples: 0 for waiting; 1 for the energy dissipation control; and 2 for feedback linearisation control.

$$E = \frac{1}{2}\dot{\theta}^2 + (\cos\theta - 1)$$

The controller proposed in Åström and Furuta (2000) has the following switching behaviours:

- *Energy dissipation phase* (phase 1): if $|E| > \epsilon$, where ϵ is a positive real number, then
$$u = \frac{\text{sign}(E)\dot{\theta}}{1 + |\dot{\theta}|}$$
- *Waiting phase* (phase 0): if $|E| \leq \epsilon$ and $|\dot{\theta}| + |\theta| > \delta$,
$$u = 0$$
- *Feedback linearisation control phase* (phase 2): if $|E| \leq \epsilon$ and $|\dot{\theta}| + |\theta| \leq \delta$,
$$u = \frac{2\dot{\theta} + \theta + \sin\theta}{\cos\theta}$$

The ranges for the initial values are set to: $|\theta(0)| \leq 19°$, $|\dot{\theta}(0)| \leq 20°/\text{s}$, the uncertainty range is given by $0.1 \leq p \leq 1.9$, i.e. $\pm 90\%$ uncertainty from the nominal value, 1, and ϵ and δ are set to 0.1 and 0.8, respectively.

An example of the controller phase switching history is shown in Figure 5. The system dynamics is highly nonlinear because of its inherent nonlinearities and the switching control. The estimated bounds are shown in Figure 6. Although it only requires to calculate the bounds for one of either sign as the system is symmetric, for the demonstration purpose, both bounds are calculated. At $t = 10s$, the bounds are between $\pm 140°$ but most of the trajectories found by Monte-Carlo simulations converge to zero. In fact, the Monte-Carlo simulation method finds only one trajectory but still far from the bound at $t = 10$s. This clearly demonstrates the advantage of the proposed bound algorithm over the blind Monte-Carlo simulations. The number of samples, N, for this example is set to 1024x10 and the one for Monte-Carlo simulations is twice more than N used. The calculation time of the presented algorithm for each instance is less than 0.5s. Monte-Carlo simulations takes significantly longer time, about 3 minutes, which would be varying depending on the number of samples, and cannot find any solution closer to the lower bounds at $t = 10$s.

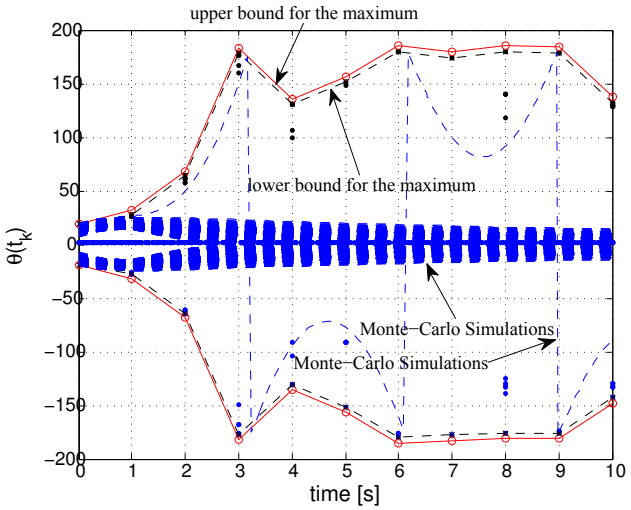

Fig. 6. Bounds for $\theta(t_k)$

5. CONCLUSIONS

An algorithm for calculating state bounds for general nonlinear systems with uncertain initial states and parameters are developed, which combines μ-formulation for optimisation problem and pseudo-LFT format. The algorithms have several advantages including: 1) no effort to obtain an LFT form is required, 2) easy to parallelise on distributed computers, and 3) the algorithm is, in fact, applicable to many types of functions including the one having finite number of discontinuity. The algorithms are applied to a simple oscillatory nonlinear discrete system, a high-dimensional biological model for ErbB signalling pathways, and a hybrid system. It is highly desirable to have numerically efficient algorithms to estimate state bounds for general nonlinear systems. Especially, the input-output robustness analysis with respect to various parametric perturbations are one of the main interest in the robustness of biological networks; Unmanned Aerial Vehicle operating in uncertain environment requires to predict the future state bounds in order to plan or re-plan its behaviour; Predicting a group of space debris is very important for the safety of any space mission. The suggested algorithm could be the main tool to analyse such complex nonlinear systems with uncertainties.

ACKNOWLEDGEMENTS

Effort sponsored by the Air Force Office of Scientific Research, Air Force Material Command, USAF, under grant number FA8655-13-1-3029. The U.S Government is authorized to reproduce and distribute reprints for Governmental purpose notwithstanding any copyright notation thereon. The authors would like to thank Lt. Col. Kevin Bollino of US-Air Force Research Laboratory for his support.

REFERENCES

Åström, K.J. and Furuta, K. (2000). Swinging up a pendulum by energy control. *Automatica*, 36(2), 287–295. doi:10.1016/s0005-1098(99)00140-5.

Acar, M., Mettetal, J.T., and van Oudenaarden, A. (2008). Stochastic switching as a survival strategy in fluctuating

environments. *Nature Genetics*, 40(4), 471–475. doi: 10.1038/ng.110. PMID: 18362885.

Balas, G.J., Doyle, J.C., Glover, K., Packard, A., and Smith, R. (2001). *μ-Analysis and Synthesis Toolbox: For Use with MATLAB, User's Guide, Version 3*. The MathWorks, Inc.

Braatz, R., Young, P., Doyle, J., and Morari, M. (1994). Computational complexity of μ calculation. *Automatic Control, IEEE Transactions on*, 39(5), 1000 –1002. doi: 10.1109/9.284879.

Cantoni, M. and Glover, K. (2000). Gap-metric robustness analysis of linear periodically time-varying feedback systems. *SIAM Journal on Control and Optimization*, 38(3), 803–822.

Chen, W.W., Schoeberl, B., Jasper, P.J., Niepel, M., Nielsen, U.B., Lauffenburger, D.A., and Sorger, P.K. (2009). Input-output behavior of ErbB signaling pathways as revealed by a mass action model trained against dynamic data. *Molecular Systems Biology*, 5. doi: 10.1038/msb.2008.74.

Clodong, S., Dhring, U., Kronk, L., Wilde, A., Axmann, I., Herzel, H., and Kollmann, M. (2007). Functioning and robustness of a bacterial circadian clock. *Molecular Systems Biology*, 3, 90. doi:10.1038/msb4100128. PMID: 17353932.

Doyle, J. (1982). Analysis of feedback systems with structured uncertainties. *IEEE Transactions on Aerospace and Electronic Systems*, 129(6), 242–250.

Doyle, J.C., Glover, K., Khargonekar, P.P., and Francis, B.A. (1989). State-space solutions to standard h_2 and h_∞ control problems. *IEEE Transactions on Automatic Control*, 34(8), 831–847.

Engelman, J.A., Zejnullahu, K., Mitsudomi, T., Song, Y., Hyland, C., Park, J.O., Lindeman, N., Gale, C.M., Zhao, X., Christensen, J., Kosaka, T., Holmes, A.J., Rogers, A.M., Cappuzzo, F., Mok, T., Lee, C., Johnson, B.E., Cantley, L.C., and Jnne, P.A. (2007). Met amplification leads to gefitinib resistance in lung cancer by activating erbb3 signaling. *Science*, 316(5827), 1039–1043. doi: 10.1126/science.1141478.

Ferreres, G. and Biannic, J.M. (2001). Reliable computation of the robustness margin for a flexible aircraft. *Control Engineering Practice*, 9, 1267–1278.

Gilchrist, M., Thorsson, V., Li, B., Rust, A.G., Korb, M., Kennedy, K., Hai, T., Bolouri, H., and Aderem, A. (2006). Systems biology approaches identify ATF3 as a negative regulator of toll-like recepter 4. *Nature*, 441(11), 173–178.

Hoehndorf, R., Dumontier, M., Gennari, J.H., Wimalaratne, S., de Bono, B., Cook, D.L., and Gkoutos, G.V. (2011). Integrating systems biology models and biomedical ontologies. *BMC systems biology*, 5(1), 124+. doi:10.1186/1752-0509-5-124.

Kao, C.Y., Megretski, A., and Jönsson, U.T. (2001). A cutting plane algorithm for robustness analysis of periodically time-varying system. *IEEE Transactions on Automatic Control*, 46(4), 579–592.

Kholodenko, B.N., Kiyatkin, A., Bruggeman, F.J., Sontag, E., and Westerhoff, H.V. (2002). Untangling the wires: A strategy to trace functional interactions in signaling and gene networks. *Proceedings of the National Academy of Sciences*, 99(20), 12841–12846.

Kim, J., Bates, D., and Postlethwaite, I. (2009). A geometrical formulation of the mu-lower bound problem. *IET Control Theory & Applications*, 3(4), 465–472. doi: 10.1049/iet-cta.2007.0391.

Kim, J., Bates, D.G., Postlethwaite, I., Ma, L., and Iglesias, P. (2006). Robustness analysis of biochemical networks models. *IEE Systems Biology*, 153(3), 96–104.

Kishida, M., Rumschinski, P., Findeisen, R., and Braatz, R.D. (2011). Efficient polynomial-time outer bounds on state trajectories for uncertain polynomial systems using skewed structured singular values. In *IEEE Multi-Conferences on Systems and Control*. Denver, CO., USA.

Kitano, H. (2004). Biological robustness. *Nat Rev Genet*, 5(11), 826–837. doi:10.1038/nrg1471.

Kuhn, C., Wierling, C., Kuhn, A., Klipp, E., Panopoulou, G., Lehrach, H., and Poustka, A. (2009). Monte Carlo analysis of an ODE Model of the Sea Urchin Endomesoderm Network. *BMC Systems Biology*, 3(1), 83+. doi: 10.1186/1752-0509-3-83.

Menon, P.P., Kim, J., Bates, D.G., and Postlethwaite, I. (2006). Clearance of nonlinear flight control laws using hybrid evolutionary optimisation. *IEEE Transactions on Evolutionary Computation*, 10(6), 689–699.

NVIDIA Developer zone: NVIDIA, CUDA 5.0 (2013). URL `http://developer.nvidia.com`.

Shinar, G., Milo, R., Martnez, M.R., and Alon, U. (2007). Input output robustness in simple bacterial signaling systems. *Proceedings of the National Academy of Sciences of the United States of America*, 104(50), 19931–19935. doi:10.1073/pnas.0706792104. PMID: 18077424.

Skogestad, S. and Postlethwaite, I. (1996). *Multivariable Feedback Control: Analysis and Design*. John Wiley & Sons Ltd.

Wagner, A. (2005). Circuit topology and the evolution of robustness in two-gene circadian oscillators. *Proceedings of the National Academy of Sciences of the United States of America*, 102(33), 11775–11780. doi: 10.1073/pnas.0501094102. PMID: 16087882.

Yonesaka, K., Zejnullahu, K., Okamoto, I., Satoh, T., Cappuzzo, F., Souglakos, J., Ercan, D., Rogers, A., Roncalli, M., Takeda, M., Fujisaka, Y., Philips, J., Shimizu, T., Maenishi, O., Cho, Y., Sun, J., Destro, A., Taira, K., Takeda, K., Okabe, T., Swanson, J., Itoh, H., Takada, M., Lifshits, E., Okuno, K., Engelman, J.A., Shivdasani, R.A., Nishio, K., Fukuoka, M., Varella-Garcia, M., Nakagawa, K., and Jnne, P.A. (2011). Activation of erbb2 signaling causes resistance to the egfr-directed therapeutic antibody cetuximab. *Science Translational Medicine*, 3(99), 99ra86. doi:10.1126/scitranslmed.3002442.

Zhao, Y.B., Kim, J., and Bates, D.G. (2011). LFT-free robustness analysis of LTI/LPTV systems. In *IEEE Multi-Conferences on Systems and Control*. Denver, CO., USA.

Zhou, W., Ercan, D., Chen, L., Yun, C.H., Li, D., Capelletti, M., Cortot, A.B., Chirieac, L., Iacob, R.E., Padera, R., Engen, J.R., Wong, K.K., Eck, M.J., Gray, N.S., and Janne, P.A. (2009). Novel mutant-selective EGFR kinase inhibitors against EGFR T790M. *Nature*, 462(7276), 1070–1074. doi:10.1038/nature08622.